J. Dairy Sci. 103
https://doi.org/10.3168/jds.2019-17604

Bovine colostrum whey: Postpartum changes of particle size distribution and immunoglobulin G concentration at different filtration pore sizes

A. Sats,[1]* T. Kaart,[2] V. Poikalainen,[3] A. Aare,[1] L. Lepasalu,[3] H. Andreson,[1] and I. Jõudu[1,4]
[1]Chair of Food Science and Technology, Estonian University of Life Sciences, Kreutzwaldi 1 Tartu, Estonia 51006
[2]Animal Breeding and Biotechnology, Estonian University of Life Sciences, Kreutzwaldi 1 Tartu, Estonia 51006
[3]Teadus ja Tegu OÜ, Aretuse 2 Märja Tartumaa 61406, Estonia
[4]Food (By-)Products Valorisation Technologies of the Estonian University of Life Sciences (VALORTECH), Kreutzwaldi 1 Tartu, Estonia 51006

ABSTRACT

Bovine colostrum, as vital as it is for calves, is also a valuable source of functional components with rich health benefits for humans. Bovine colostrum whey consists of a large number of bioactive proteins and peptides. The most abundant of these is IgG. Particle size distribution (PSD) is an important feature of many of the processes in the dairy food industries. Despite this, scientific literature on PSD of colostrum whey is scarce. The goal of this research was to describe bovine colostrum whey PSD with an emphasis on postpartum milking time, filtration (pore size 450, 100, and 20 nm), IgG concentration, and lactation number. For this purpose, 4 postpartum milking colostrum samples were sequentially milked from 46 Holstein cows at 12 ± 1 h intervals. Colostrum whey was prepared by renneting and diluted (1:200) for PSD analyses by a Malvern Zetasizer Nano ZS (Malvern Instruments Ltd., Malvern, UK). Immunoglobulin G concentration of these diluted colostrum whey samples were analyzed by an Octet K2 (Molecular Devices LLC, San Jose, CA) system. Linear mixed model analysis revealed significant effects of filter pore size, postpartum milking, and lactation on colostrum whey IgG concentrations. The percentage of particles in the size interval 5 to 15 nm (the hydrodynamic diameter of IgG is around 10 nm) had an intermediate positive correlation ($r = 0.50$) with IgG concentration. Furthermore, we showed that PSD was associated with IgG concentration, postpartum milking time, and lactation number. The PSD measurement results showed the mean hydrodynamic diameter of 100 nm pore size filtered colostrum whey to be around 10 nm. This, with the IgG concentration results, suggests that even though the size of IgG is around 10 nm, a 100 nm pore size is adequate for membrane-involved IgG separations. In terms of energy efficiency of the filtration process, the use of a larger filter pore size can make a remarkable difference, for example, in pressurizing and cooling costs. Our work contributes to the development of sustainable and widely available colostrum-derived food and feed supplements.
Key words: bovine colostrum whey, particle size distribution, immunoglobulin G, filtration pore size

INTRODUCTION

Colostrum is a mammary gland secretion already formed before and then secreted in the first days after parturition (Blättler et al., 2001). Ensuring that a calf receives high-quality colostrum straight after its birth is widely recognized to be crucial to a calf's health and survival (Stott et al., 1979; Godden, 2008). Calf well-being, however, can be limited by its ability to consume a sufficient amount of colostrum. Shortage of high-quality colostrum is a particular problem on small-scale dairy and beef cattle farms, whereas large-scale dairy farms have an excess of colostrum on a daily basis (Kehoe et al., 2007). A possible solution for low-quality or deficient colostrum is to fortify the low-quality colostrum or milk with concentrated colostrum whey proteins (Lago et al., 2018). Bovine colostrum-based feed supplements can also be useful in other areas of animal husbandry or as pet feed supplements. For example, administrating freeze-dried bovine colostrum whey to weaned piglets has a beneficial effect on their growth and feed efficiency (Boudry et al., 2008). Furthermore, an increasing demand for functional and nutraceutical foods has encouraged food-processing industries to develop high-value products with additional health benefits. The need for such products is most urgent in developing and underdeveloped nations that often struggle with high child mortality rates that could be reduced by the use of bovine colostrum-derived products (Borad and Singh, 2018).

Bovine colostrum and its whey form a complex matrix consisting of a large number of components with various functionalities and properties. The most abundant

Received September 18, 2019.
Accepted April 6, 2020.
*Corresponding author: Andres.Sats@emu.ee

component of colostrum whey is IgG (Korhonen et al., 2000). Unfortunately, the raw state of immunoglobulins is thermo-labile, which can lead to a loss of functionality and to a pudding-like consistency (Meylan et al., 1996; Godden et al., 2003; Elizondo-Salazar et al., 2010). Therefore, conventional milk preservation and concentration technologies are often not suitable for colostrum processing.

The challenges of processing and preserving colostrum have led to numerous reports on different processing technologies. Borad and Singh (2018) classified these technologies as chemical preservation, freezing, thermal preservation, drying, and emerging food-processing techniques (membrane and high-pressure processing; pulsed electric field and irradiation). Particle size distribution (**PSD**) is important in all of these technologies. Membrane processing is efficient and sustainable as it can derive specific separations at room temperature. Unfortunately, the separation is dependent on the combined effects of membrane and retained material deposited layer, which acts as a secondary membrane. Seemingly, the PSD relates to pore size. The pore size in turn affects the membrane flux (amount of permeate produced per area of membrane surface per time) as an important operating parameter. Put simply, larger pore size enables higher flux and lower energy demand for pressurizing and cooling the filtration substance. So far, membrane processing of colostrum was based on the molecular weights of its components (Elfstrand et al., 2002; Pouliot and Gauthier, 2006). However, PSD can be a useful tool in choosing or optimizing membrane-processing operating parameters (Heidebrecht et al., 2018b; Heidebrecht and Kulozik, 2019). Furthermore, membrane technologies in combination with chromatography (Gagnon et al., 2015; Zydney, 2016; Heidebrecht et al., 2018a) or other methods such as selective precipitation-assisted recovery (Venkiteshwaran et al., 2008) are found to be very useful for the purification of immunoglobulins from biological fluids.

The polydispersity of the sample affects the dynamic light scattering (**DLS**) particle size measurement (Baalousha and Lead, 2012). In multimodal and wide range size distributions, the sub-distribution of smaller particles tends to shift toward bigger particles. The extent of this shift is dependent on the difference between the sub-distributions. Filtration can be a suitable tool for reducing the effect of polydispersity.

Recently, Heidebrecht and Kulozik (2019) reported PSD of isolated or purified whey proteins measured by DLS. However, when studying PSD of whole colostrum whey, the rapid changes in the postpartum timeline (Elfstrand et al., 2002) and the polydispersity are substantial. The aim of this work was to study colostrum whey PSD with an emphasis on changes in the postpartum timeline, the filtration pore size (450, 100, and 20 nm), the IgG concentration, and the lactation number.

MATERIALS AND METHODS

Sample Collection

Four postpartum milking colostrum samples from 46 Holstein cows (n = 184) were collected from the Experimental Farm of the Estonian University of Life Sciences during a 2-yr period (2015–2016). After parturition, calves were separated from their dams to prevent suckling. Cows were milked for the first time between 30 and 120 min after parturition with a portable milking machine. Thereafter, cows were milked twice daily at regular milking times (at 12 ± 1 h intervals). Composite samples (50 mL) were frozen and stored immediately at −20°C. Of the 46 studied cows, 10 started their first, 8 their second, 9 their third, 9 their fourth, and 10 their fifth or sixth lactations; in later statistical analyses the third and later lactations were considered together due to the similarity of the PSD and IgG concentration, and their changes. Previous lactation yield was 9,692 ± 1,894 kg (n = 36; mean ± SD) with 373.0 ± 76.5 kg of fat and 320.4 ± 58.7 kg of protein production during 295.8 ± 12.6 d in lactation.

Sample Preparation

Colostrum whey was prepared by renneting with Naturen Stabo 230 (Chr. Hansen Holding A/S, Hoersholm, Denmark) at 34°C for 40 min before curd cutting. For whey collection, the curd was drained with a stainless steel sieve (pore size 1 mm). The whey obtained was diluted by a factor of 1:200 with RPMI (Roswell Park Memorial Institute) 1640 medium (pH 7.0) (PAA Laboratories GmbH, Pasching, Austria) as described by Mootse et al. (2014). Before particle size and IgG measurements, 10 mL of the diluted samples were filtered stepwise with 450, 100, and 20 nm pore size syringe filters (Whatman GmbH, Dassel, Germany). After PSD measurement, the 1.5-mL samples were frozen and stored at −20°C for IgG analysis.

Measurement of Particle Size Distribution

Dynamic light scattering analyses were performed at 20°C in 4 consequent measurements using a Zetasizer Nano ZS analyzer (Malvern Instruments Ltd., Malvern, UK) equipped with a 633 nm He-Ne laser, similar to the procedure described by Mootse et al. (2014). The particle size distribution was determined at a fixed 173°

backscattered angle using the default protein analysis mode with automatic duration and attenuation selection.

Measurement of IgG

The IgG measurements were conducted with the Octet K2 (Molecular Devices LLC, San Jose, CA) biolayer interferometry protocol using 2 sensors in one full measurement round. Protein G (Pro G) sensors were equilibrated off-line in a kinetic buffer [0.01 *M* PBS, pH 7.4 (Gibco, Gaithersburg, MD, cat. no. 14190); 0.1% BSA (PAN-Biotech GmbH, Aidenbach, Germany, cat. no. P06-1391500); 0.02% Tween 20 (Carl Roth GmbH and Co. KG, Karlsruhe, Germany, art. no. 9127.1); 0.1% Proclin 300 (Sigma-Aldrich, Saint Louis, MO, cat. no. 48914-U)] for 10 min and then regenerated with a regeneration buffer (0.1 *M* glycine buffer, pH 1.7) and a kinetic buffer for 30 s at 200 rpm (3 cycles, 1 cycle consisting of the sensor being incubated in the regeneration buffer for 5 s following an incubation in the kinetic buffer for 5 s). After regeneration, sensors were transferred to IgG standards or bovine colostrum milk samples (diluted in kinetic buffer) for 120 s at 200 rpm. Immunoglobulin G standards 80, 40, 20, 10, 5, 2.5, and 1.25 (μg/mL) were prepared from a Sigma-Aldrich product (catalog 15506, 10 mg, IgG from bovine serum, lot #SLBM2612V). The raw samples consisted of 99.5% RPMI 1640 and 0.5% whey from bovine colostrum. For quantification, all samples were diluted 5 and 25 times, respectively. For comparison with previous studies, the IgG concentrations were recalculated with a dilution factor (0.005 vol/vol) used for PSD analyses.

Statistical Analyses

The filter pore size, postpartum milking, and lactation number were considered as categorical factors and their effects on filtered colostrum whey IgG concentration were analyzed by fitting a general linear mixed model. In this model, fixed effects of the above factors and their interactions, and random effect of cow were considered. The marginal means (least squares means with 95% confidence interval) were estimated and compared by filter pore size values, milkings, and lactation numbers applying the Tukey test for multiple testing. The magnitude of the cow effect was estimated using the intraclass correlation coefficient (**ICC**).

For statistical analyses, the PSD in the form of frequency tables obtained from Zetasizer Nano ZS analyzer (Malvern Instruments Ltd., Malvern, UK) software version 7.11, were used. In these tables particle sizes from 0.1 to 1,000 nm were divided into 200 equal intervals on a $\log_{10}$-scale and the particles' volume percentage in each size interval was calculated. Therefore, for each sample 200 numerical values representing its PSD was obtained. These values were used to calculate the mean PSD for postpartum milking, lactation number, and filter pore size, and to perform the principal component analysis (**PCA**) to discover common PSD patterns. General linear mixed models with principal components as dependent variables that considered the fixed effects of these factors and their interactions as well as the random effect of the cow were used to analyze to what extent these patterns reflect the differences between the filtering pore size values, milkings, and lactation numbers. The resulting PSD was also used to estimate the linear correlation coefficient between samples' IgG concentrations and particle frequency in each size interval.

Finally, the particle size interval of 5 to 15 nm, more positively related to the IgG concentration, was selected and the total frequency of particles in this interval as well the PSD mode were calculated. The relationships between the calculated characteristics and the sample's IgG concentration were studied with linear correlation analysis and the potential nonlinear relationships were fitted with a locally weighted scatterplot smoothing curve.

All statistical analyses (significance was declared at $P \leq 0.05$) were performed and all figures were constructed with R version 3.5.1 (R Foundation for Statistical Computing, Vienna, Austria). For modeling the packages "car," "lme4," "lsmeans," and "multcompView" and for PCA the package "ade4" were used.

RESULTS AND DISCUSSION

PSD of Colostrum Whey IgG

PSD and Hydrodynamic Diameter of IgG. The mean PSD of bovine colostrum whey at different filtration pore sizes depending on postpartum milking are shown in Figure 1 (and Supplemental Figures S1 and S2; https://doi.org/10.3168/jds.2019-17604). Irrespective of the filtration pore size from the first 2 milkings, at least 50% of the particles had sizes between 5 and 15 nm with a median in the interval of 8.5 to 10.7 nm. This is consistent with the fact that IgG is the most abundant component of colostrum whey (Korhonen et al., 2000). It is also in agreement with Heidebrecht and Kulozik (2019), who reported 10.67 nm as the median of bovine IgG size distribution and with Ahrer et al. (2003, 2006), who described the hydrodynamic diameter of human IgG to be around of 10 nm. Furthermore, according to Pouliot and Gauthier (2006) IgG is distinguishable by the molecular weights of other major components present in whey, being roughly twice as heavy as serum albumin, lactoperoxidase, and lactofer-

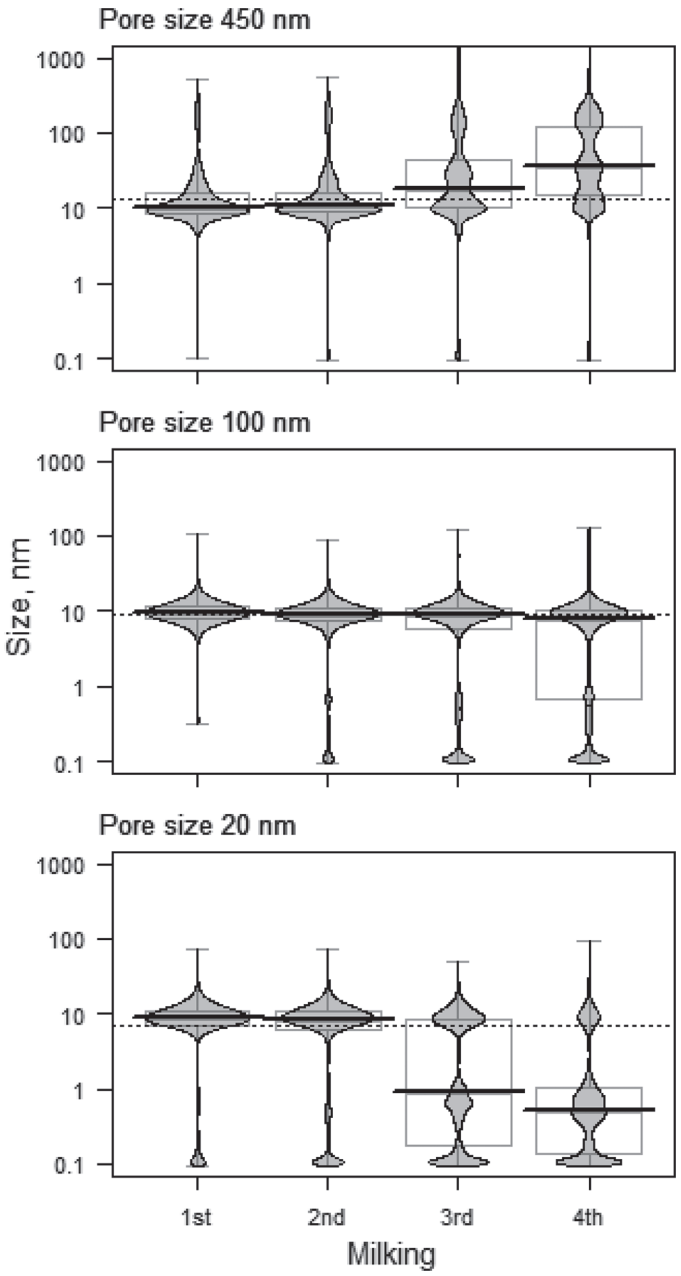

Figure 1. Bean plots showing the particle size distribution (PSD) of bovine colostrum whey at different filtration pore sizes (450, 100, and 20 nm) for the first 4 postpartum milkings. Each distribution presents the mean PSD of samples from 46 cows, and the particle size axes are shown on a $\log_{10}$-scale. Gray boxes denote the area of the middle 50% of particle sizes, error bars indicate the range of particle sizes, strong black lines mark the median particle size by milkings, and dotted lines mark the median particle size over 4 milkings.

rin; and at least 3 times as heavy as α-LA, β-LG, and several growth factors.

PSD and IgG Correlations. The correlation analysis of IgG concentration in whey and PSD showed the strongest positive correlations around 10 nm (Figure 2A). The percentage of particles in the size interval 5 to 15 nm had a statistically significant positive correlation with IgG concentration ($r = 0.50$, $P < 0.001$). This relationship is also characterized by similar changes in 5 to 15 nm particle frequency with different factors; the frequency was higher in the case of filter pore sizes of 100 and 450 nm, at first milkings, and for later lactations (Supplemental Figure S3; https://doi.org/10.3168/jds.2019-17604). More detailed localization of the IgG concentration related to particle sizes showed that particle size mode in the interval 5 to 15 nm (with a mean value of 8.5 nm) was weakly correlated ($r = 0.27$, $P < 0.001$) with the IgG concentration, whereas nonlinear smoothing indicated only slightly higher IgG concentrations in the case of the PSD mode in the interval 8 to 10 nm (Figure 2B). These results are in agreement with Heidebrecht and Kulozik (2019), who reported IgG PSD hydrodynamic diameter percentiles 10, 50, and 90 to be 7.86, 10.67, and 15.33 nm, respectively.

Filtration Pore Size—PSD and IgG Concentration

PSD and Filtration Pore Size. In the 450 nm pore size samples, larger particle sub-distributions (20–60 and 100–300 nm) appeared in the postpartum timeline (Figure 1 and Supplemental Figure S1; https://doi.org/10.3168/jds.2019-17604). The hydrodynamic diameter of the casein micelle is around 200 nm (Mootse et al., 2014; Heidebrecht and Kulozik, 2019). Therefore, 100 to 300 nm range sub-distributions might represent the remnant casein micelles or their fractions. The 20 to 60 nm sub-distribution might represent IgM or IgA, as according to Heidebrecht and Kulozik (2019) the hydrodynamic diameters of IgM and IgA are in the range of 19 to 30 nm and 14 to 25 nm, respectively. However, this explanation is questionable, because as reported by Elfstrand et al. (2002), the concentrations of bovine colostrum IgM and IgA are about 20 and 50 times lower compared with IgG and decrease in the postpartum timeline at a similar pace. Most likely, the 20 to 60 nm sub-distributions (Figure 1 and Supplemental Figure S1; https://doi.org/10.3168/jds.2019-17604) illustrate the combination of a decrease in IgG concentration and a polydispersity of samples, as the "size shifting" effect induced by the bigger particles (100–300 nm) on the smaller particles (5–15 nm) increases while the IgG concentration decreases (Figure 3). The disappearance of the 20 to 60 nm sub-distribution after 100 nm pore size filtration also supports this "size shifting" claim. As the filtration pore size decreases, the 0.1 to 1 nm range sub-distributions increase. This increase can be explained by the removal of bigger particles, which allows better detection of smaller particles, and by the loss of IgG (Supplemental Table S1; https://doi.org/

10.3168/jds.2019-17604). The hydrodynamic diameter of lactose particles is around 1 nm (Pisponen et al., 2016). Regardless of the steady increase of the lactose content over the postpartum timeline (McGrath et al., 2016), we can conclude that in case of the 20 and 100 nm pore size PSD, the increase of the 0.1 to 1 nm range sub-distribution (Figure 1) also reflects the decrease in IgG concentration (Figure 3). This suggests that polydispersity, as an undesired phenomenon that affects the precision of DSL measurements, might also be a useful tool. For example, when the concentration of component(s) in one sub-distribution is constant, it is possible to estimate the content changes of other component(s) by their sub-distribution proportion changes.

IgG Concentration and Filtration Pore Size. Linear mixed model analysis revealed significant ($P < 0.001$) effects of filter pore size, postpartum milking, and lactation number on sample IgG concentration (Figure 3 and Supplemental Table S1; https://doi.org/10.3168/jds.2019-17604). The mean IgG concentration over all milkings and lactation numbers at a 20 nm filter pore size was 2.8 mg/mL lower compared with a 100 nm filter pore size (14.9 mg/mL, $P = 0.009$) and 4.6 mg/mL lower compared with a 450 nm filter pore size (16.8 mg/mL, $P < 0.001$); the difference between 450 and 100 nm filter pore sizes was nonsignificant ($P = 0.110$). This suggests a significant IgG loss at a 20 nm pore size filtration, whereas the differences between filter pore sizes are similar irrespective of the milking and lactation numbers ($P = 0.300$ and $P = 0.749$, respectively). Lower IgG content in 20 nm pore size samples and the fact that the mean hydrodynamic diameter of 100 nm pore size filtered colostrum whey is around 10 nm suggests that a 100 nm pore size is most suitable for membrane-involved IgG separation. Even though the difference between 20 and 100 nm might not seem much in terms of energy consumption (pressurizing and cooling), the use of a 5-fold larger filter pore size makes a remarkable difference. However, we suggest that filtration has the greatest potential particularly in combination with further refining method. Hence, the cost effectiveness (including minimum IgG concentration worth separating) is dependent on that "further refining" method and several other aspects such as availability and quality of the raw material, production scale, input costs, and so on.

Postpartum Milking—PSD and IgG Concentration

PSD in the Postpartum Timeline. The most evident changes appear in the PSD of the third and fourth milkings (Figure 1 and Supplemental Figure S1; https://doi.org/10.3168/jds.2019-17604) as the share of IgG sub-distribution (around 10 nm) decreases, whereas other sub-distributions increase in the postpartum timeline. Interestingly, when comparing the PSD of the 100 and 20 nm pore size samples (Figure 1), the IgG sub-distribution decrease and the 0.1 to 1 nm size range sub-distribution increase are far more apparent in the 20 nm pore size samples. In theory, the IgG sub-distributions (as largest particles in both pore size samples)

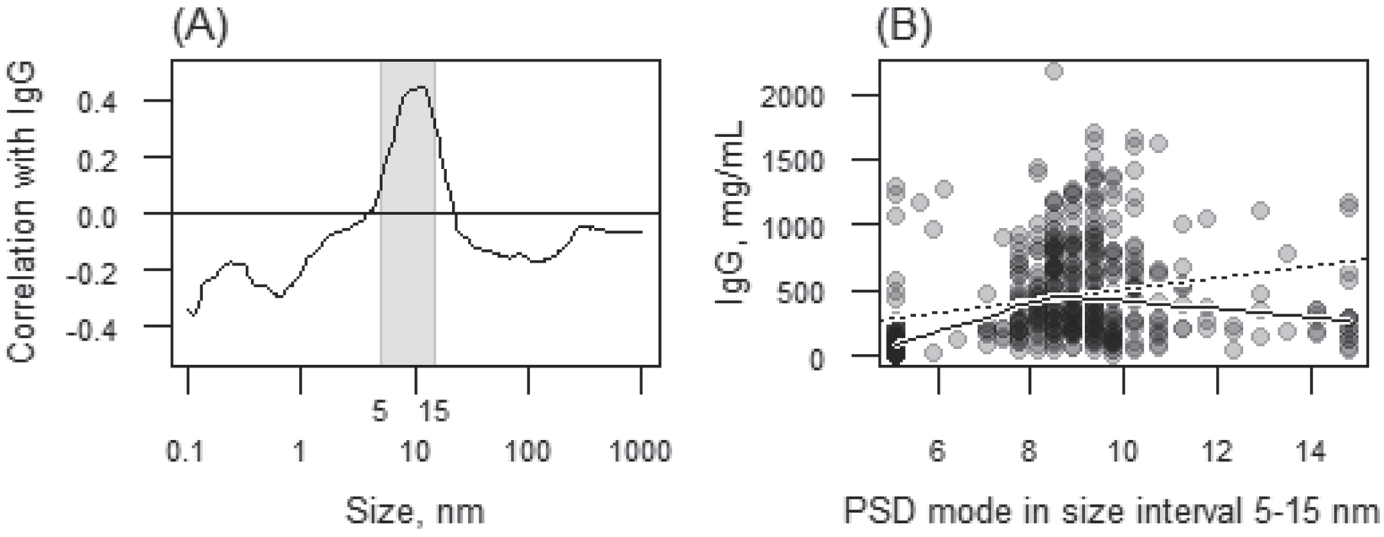

Figure 2. (A) Correlation between bovine colostrum whey IgG concentration and particle size distribution (PSD; all correlations with absolute value >0.1 are statistically significant, $P < 0.05$); the gray rectangle indicates the sub-distribution of IgG in the range of 5 to 15 nm. (B) Relationship between the PSD mode in the size interval 5 to 15 nm and IgG concentration; each of the points represents one sample, and dotted and solid lines denote the linear relationship and smoothed nonlinear relationship, respectively, fitted with a locally weighted scatterplot smoothing curve.

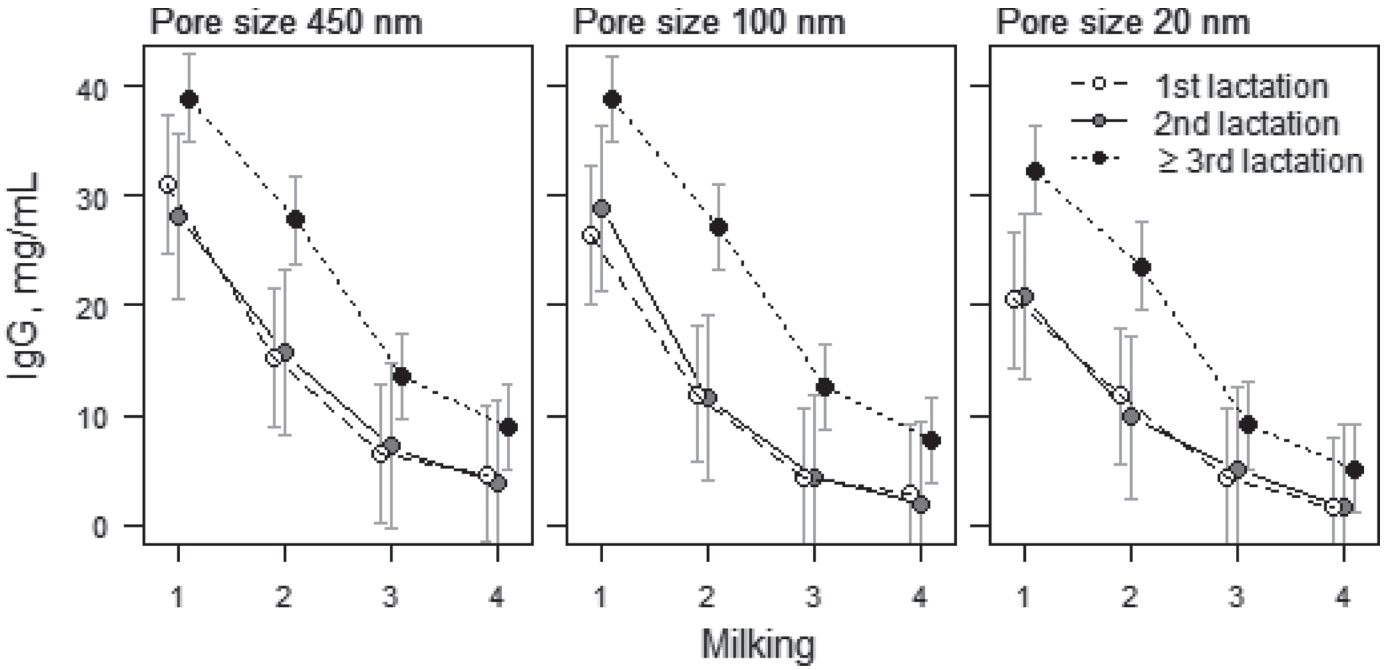

Figure 3. Bovine colostrum whey IgG (mg/mL) by filter pore size, postpartum milking, and lactation number. Presented are the LSM with 95% CI according to the linear mixed model considering fixed effects of filter pore size, postpartum milking, lactation number, and all their interactions as well as the random effect of cow. All main effects and postpartum milking by lactation number interaction effects were statistically significant (all $P < 0.001$).

should dominate both pore size PSD. Therefore, the only rational explanation for these PSD differences is an IgG loss during the 20 nm filtration (Figure 3 and Supplemental Table S1; https://doi.org/10.3168/jds.2019-17604). Furthermore, when comparing IgG concentration (Supplemental Table S1; https://doi.org/10.3168/jds.2019-17604) with corresponding PSD (Figure 1), the PSD seems to reflect even minor IgG concentration changes. Hence, the PSD of colostrum whey shows an IgG decrease both in the postpartum timeline as well as in the filtration loss.

IgG Concentration in the Postpartum Timeline. The mean IgG concentration in the first milking samples (29.5 mg/mL) is significantly higher compared with subsequent milkings (17.2, 7.4, and 4.3 mg/mL, respectively) at any of the filter pore sizes and all lactations (all $P < 0.05$). The rate of decrease in the IgG concentration slows down with time (Figure 3 and Supplemental Table S1; https://doi.org/10.3168/jds.2019-17604). This is in agreement with the general finding that IgG concentration decreases in the postpartum timeline (Phipps et al., 2017; Silva-del-Rio et al., 2017; Raimondo et al., 2019). Overall, the concentration was within a similar range (Supplemental Table S1; https://doi.org/10.3168/jds.2019-17604) to that of colostrum whey obtained by Elfstrand et al. (2002), of 18.8 mg/mL for a mixture of 0 to 80 h postpartum samples.

Lactation Number—PSD and IgG Concentration

PSD and Lactation Number. Compared with the third and later lactations, the share of the 0.1 to 1 nm size range sub-distribution increases with milking number in earlier lactation samples (Figure 4 and Supplemental Figure S2; https://doi.org/10.3168/jds.2019-17604). Interestingly, the PSD of the third and later lactations (Figure 4) are very similar to the overall 100 nm pore size PSD (Figure 1). This resemblance can be explained by the fact that the third and later lactation sample(s) represent the majority (28 out of 46) of the sampled cows. In addition, it seems that in the case of higher IgG concentrations (later lactations) the PSD does not reflect the IgG decrease as evidently as in lower concentrations. This suggests that PSD reflects the IgG concentration most clearly at certain proportions between IgG and a 0.1 to 1 nm size range (lactose) sub-distribution.

IgG Concentration and Lactation Number. Higher mean IgG concentration of the older (≥third lactation) cows (Figure 3) is significant ($P < 0.05$) for all filter pore sizes only at the first and second milking (Supplemental Table S1; https://doi.org/10.3168/jds.2019-17604). Later in the postpartum timeline, particularly between the second and the third milking, the IgG concentration decreases faster in older cows

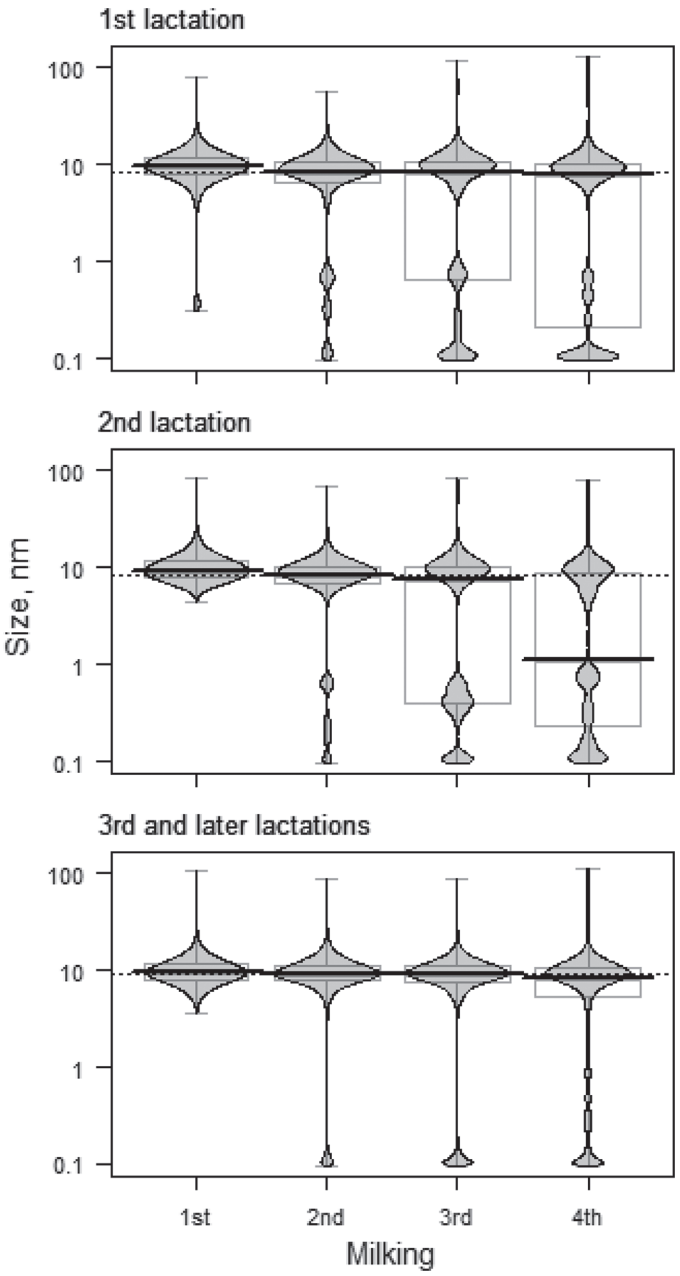

Figure 4. Bean plots representing the particle size distribution (PSD) of bovine colostrum whey at filtration pore size 100 nm at the first 4 postpartum milkings depending on lactation number (first lactation n = 10, second lactation n = 8, third and later lactations n = 28). Each distribution shows the mean PSD and particle size axes presented on a $\log_{10}$-scale; gray boxes denote the area of the middle 50% of particle sizes, error bars indicate the range of particle sizes, strong black lines mark the median particle size by milkings, and dotted lines mark a median particle size over 4 milkings.

(significant milking by lactation interaction effect, $P < 0.001$). This faster decrease might link to the finding that initially, in the first and second milking, the IgG concentrations in older cows' colostrum whey are significantly higher compared with younger cows. Lower IgG content in the first and second lactations is in good agreement with the findings of Kehoe et al. (2011) and Dunn et al. (2017). Currently, the ICC of the random cow effect (ICC = 0.451) indicates that 45.1% of the total variance in IgG concentration is caused by the differences between cows (i.e., is cow specific). Hence, even though the mean IgG concentration in colostrum whey from first or second lactation cows is lower (Figure 3), it should not be automatically discarded as being of low quality.

Principal Component Analyses

The PCA revealed one strong pattern in PSD, explaining 44.0% of the particle size variability. This pattern (the first principal component, **PC1**) indicates that most of the variability of single sample PSD is caused by the differences in particle size frequencies around 10 nm and in the intervals 0.1–0.2 and 0.9–1 nm (Figure 5A). Such a result can be expected because these are the most frequent size ranges of particles (cf. Figures 1 and 3). As PSD is expressed as a scale of relative frequencies, it is logical (and in accordance with the results discussed above), that PC1 is positively associated with particle sizes of around 10 nm, and negatively associated with particle sizes of less than 1 nm (an increase in one size range must necessarily reduce the frequencies in another size range). The PC1 considers simultaneously the differences between filter pore sizes, postpartum milkings, and lactations (effects of all these factors on PC1 were statistically significant, at $P < 0.001$; Figures 5B–D). The random cow effect explains 14.4% of the variability of PC1, indicating that the particle size ranges related to PC1 are animal specific (Figure 5E). This is consistent with the high variability of colostrum quality (i.e., its IgG content; Bielmann et al., 2010; Elsohaby et al., 2017), which in turn is reflected in the PSD. The second strongest pattern (the second principal component) explained 15.9% of the particle size variability, which contrasts the frequency of particles with sizes over and under 15 nm (Figure 5A) and mainly distinguishes the samples according to filter pore size: 450 nm versus 20 and 100 nm (Figures 1 and 5B). This 15 nm differentiation is in agreement with earlier IgG hydrodynamic diameter measurement results (Ahrer et al., 2003, 2006; Heidebrecht and Kulozik, 2019) and corroborates the finding that the 100 nm pore size is suitable for immunoglobulin separation from bovine colostrum whey.

CONCLUSIONS

This study provides a better understanding of bovine colostrum whey, describing the PSD at 450, 100, and 20

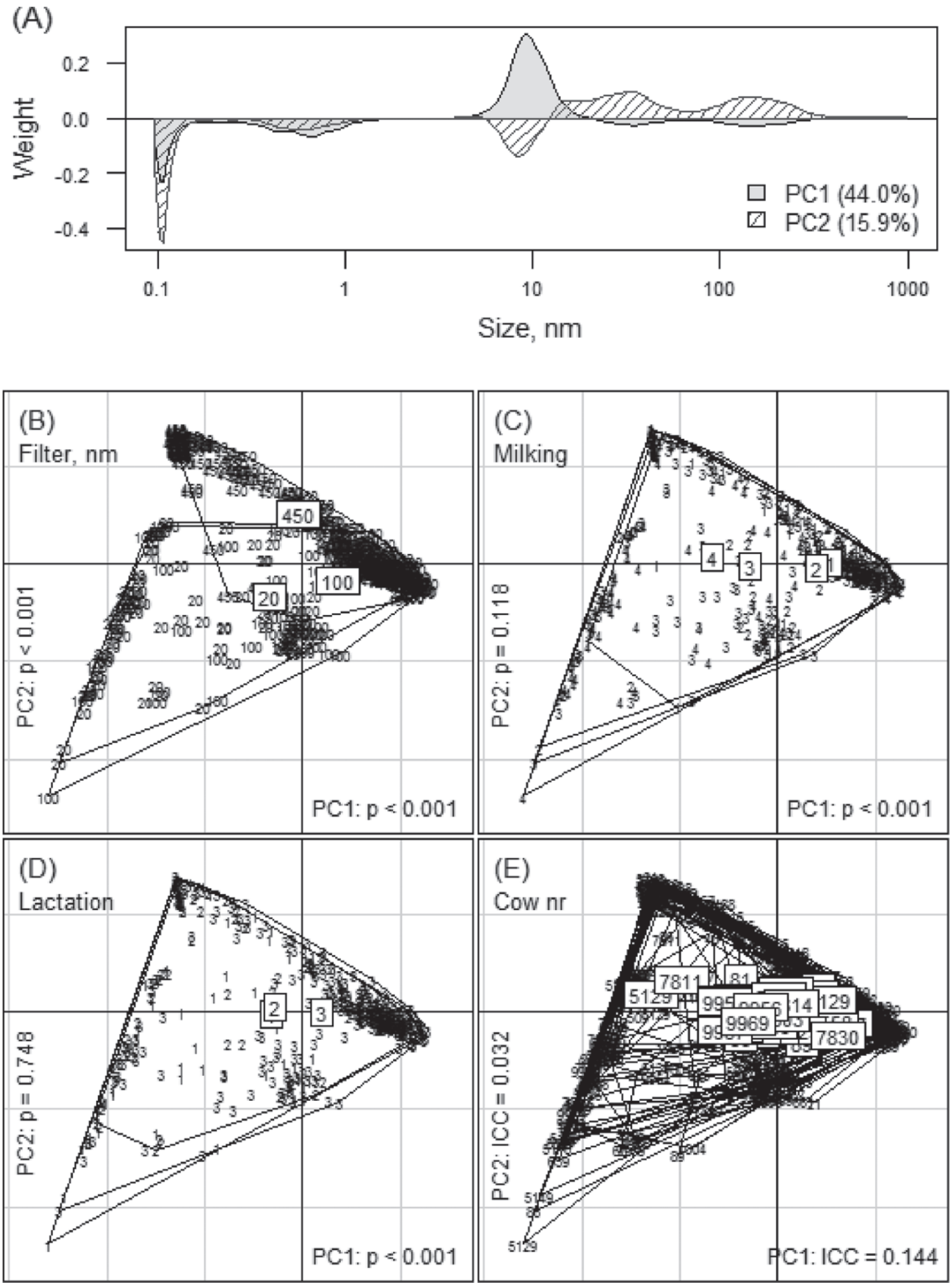

Figure 5. Results of the principal component (PC) analysis of particle size distributions in the interval 0.1 to 1,000 nm. (A) The weights (eigenvectors) of different particle size subinterval frequencies in the first 2 PC. (B)–(E) Location of samples according to their first 2 PC scores sorted by filter pore size, milking, lactation number, and cow. Each sample is marked with its group symbol and samples from the same group are surrounded with a line. Higher values in boxes mark the groups' centroids, and *P*-values denote the significance of the factors according to the linear mixed model considering fixed effects of filter pore size, milking, and lactation number as well as random effect of cow. For the random cow effect, the proportion of variance of PC scores considered by the cow effect (intraclass correlation coefficient, ICC) is presented; for both PC, separate models were fitted.

nm filtration pore sizes with an emphasis on IgG concentration, postpartum milking, and lactation number of cows. It also demonstrates that when applying sample filtration, DLS is suitable for PSD estimation even in complex and high polydispersity matrices such as colostrum whey. The PSD of colostrum whey with the IgG concentration results show that for membrane-involved separation of IgG with hydrodynamic diameter around 10 nm, the 100 nm pore size is adequate. Hence, 100 nm filtration has great potential as a low-cost method for initial separation of IgG from colostrum whey, following an additional refining method. Further studies that combine membrane-involved separation with recent discoveries are required to provide cost-effective colostrum as the need for widely available high-value nutraceuticals is constantly growing.

ACKNOWLEDGMENTS

This work was supported by the European Union's Horizon 2020 research and innovation programme under grant agreement No. 810630 "ERA Chair for Food (By-) Products Valorisation Technologies of the Estonian University of Life Sciences (VALORTECH)" and the Estonian University of Life Sciences research and development base financing (P170195VLTQ). The authors declare no conflict of interest.

REFERENCES

Ahrer, K., A. Buchacher, G. Iberer, D. Josic, and A. Jungbauer. 2003. Analysis of aggregates of human immunoglobulin G using size exclusion chromatography, static and dynamic light scattering. J. Chromatogr. A 1009:89–96. https://doi.org/10.1016/S0021-9673(03)00433-3.

Ahrer, K., A. Buchacher, G. Iberer, and A. Jungbauer. 2006. Thermodynamic stability and formation of aggregates of human immunoglobulin G characterised by differential scanning calorimetry and dynamic light scattering. J. Biochem. Biophys. Methods 66:73–86. https://doi.org/10.1016/j.jbbm.2005.12.003.

Baalousha, M., and J. R. Lead. 2012. Rationalizing nanomaterial sizes measured by atomic force microscopy, flow field-flow fractionation, and dynamic light scattering: Sample preparation, polydispersity, and particle structure. Environ. Sci. Technol. 46:6134–6142. https://doi.org/10.1021/es301167x.

Bielmann, V., J. Gillan, N. R. Perkins, A. L. Skidmore, S. Godden, and K. E. Leslie. 2010. An evaluation of Brix refractometry instruments for measurement of colostrum quality in dairy cattle. J. Dairy Sci. 93:3713–3721. https://doi.org/10.3168/jds.2009-2943.

Blättler, U., H. M. Hammon, C. Morel, C. Philipona, A. Rauprich, V. Rome, I. Le Huerou-Luron, P. Guilloteau, and J. W. Blum. 2001. Feeding colostrum, its composition and feeding duration variably modify proliferation and morphology of the intestine and digestive enzyme activities of neonatal calves. J. Nutr. 131:1256–1263. https://doi.org/10.1093/jn/131.4.1256.

Borad, S. G., and A. K. Singh. 2018. Colostrum immunoglobulins: Processing, preservation and application aspects. Int. Dairy J. 85:201–210. https://doi.org/10.1016/j.idairyj.2018.05.016.

Boudry, C., J. P. Dehoux, J. Wavreille, D. Portetelle, A. Théwis, and A. Buldgen. 2008. Effect of a bovine colostrum whey supplementation on growth performance, faecal *Escherichia coli* population and systemic immune response of piglets at weaning. Animal 2:730–737. https://doi.org/10.1017/S175173110800164X.

Dunn, A., A. Ashfield, B. Earley, M. Welsh, A. Gordon, and S. J. Morrison. 2017. Evaluation of factors associated with immunoglobulin G, fat, protein, and lactose concentrations in bovine colostrum and colostrum management practices in grassland-based dairy systems in Northern Ireland. J. Dairy Sci. 100:2068–2079. https://doi.org/10.3168/jds.2016-11724.

Elfstrand, L., H. Lindmark-Mansson, M. Paulsson, L. Nyberg, and B. Akesson. 2002. Immunoglobulins, growth factors and growth hormone in bovine colostrum and the effects of processing. Int. Dairy J. 12:879–887. https://doi.org/10.1016/S0958-6946(02)00089-4.

Elizondo-Salazar, J. A., B. M. Jayarao, and A. J. Heinrichs. 2010. Effect of heat treatment of bovine colostrum on bacterial counts, viscosity, and immunoglobulin G concentration. J. Dairy Sci. 93:961–967. https://doi.org/10.3168/jds.2009-2388.

Elsohaby, I., J. T. McClure, M. Cameron, L. C. Heider, and G. P. Keefe. 2017. Rapid assessment of bovine colostrum quality: How reliable are transmission infrared spectroscopy and digital and optical refractometers? J. Dairy Sci. 100:1427–1435. https://doi.org/10.3168/jds.2016-11824.

Gagnon, P., R. Nian, Y. Yang, Q. Yang, and C. L. Lim. 2015. Non-immunospecific association of immunoglobulin G with chromatin during elution from protein A inflates host contamination, aggregate content, and antibody loss. J. Chromatogr. A 1408:151–160. https://doi.org/10.1016/j.chroma.2015.07.017.

Godden, S. 2008. Colostrum management for dairy calves. Vet. Clin. North Am. Food Anim. Pract. 24:19–39. https://doi.org/10.1016/j.cvfa.2007.10.005.

Godden, S. M., S. Smith, J. M. Feirtag, L. R. Green, S. J. Wells, and J. P. Fetrow. 2003. Effect of on-farm commercial batch pasteurization of colostrum on colostrum and serum immunoglobulin concentrations in dairy calves. J. Dairy Sci. 86:1503–1512. https://doi.org/10.3168/jds.S0022-0302(03)73736-9.

Heidebrecht, H.-J., B. Kainz, R. Schopf, K. Godl, Z. Karcier, U. Kulozik, and B. Förster. 2018a. Isolation of biofunctional bovine immunoglobulin G from milk- and colostral whey with mixed-mode chromatography at lab and pilot scale. J. Chromatogr. A 1562:59–68. https://doi.org/10.1016/j.chroma.2018.05.046.

Heidebrecht, H.-J., and U. Kulozik. 2019. Fractionation of casein micelles and minor proteins by microfiltration in diafiltration mode. Study of the transmission and yield of the immunoglobulins IgG, IgA and IgM. Int. Dairy J. 93:1–10. https://doi.org/10.1016/j.idairyj.2019.01.009.

Heidebrecht, H.-J., J. Toro-Sierra, and U. Kulozik. 2018b. Concentration of immunoglobulins in microfiltration permeates of skim milk: Impact of transmembrane pressure and temperature on the IgG transmission using different ceramic membrane types and pore sizes. Foods 7:101. https://doi.org/10.3390/foods7070101.

Kehoe, S. I., A. J. Heinrichs, M. L. Moody, C. M. Jones, and M. R. Long. 2011. Comparison of immunoglobulin G concentrations in primiparous and multiparous bovine colostrum. Prof. Anim. Sci. 27:176–180. https://doi.org/10.15232/S1080-7446(15)30471-X.

Kehoe, S. I., B. M. Jayarao, and A. J. Heinrichs. 2007. A Survey of bovine colostrum composition and colostrum management practices on Pennsylvania dairy farms. J. Dairy Sci. 90:4108–4116. https://doi.org/10.3168/jds.2007-0040.

Korhonen, H., P. Marnila, and H. S. Gill. 2000. Milk immunoglobulins and complement factors. Br. J. Nutr. 84(Suppl 1):75–80. https://doi.org/10.1017/S0007114500002282.

Lago, A., M. Socha, A. Geiger, D. Cook, N. Silva-del-Rio, C. Blanc, R. Quesnell, and C. Leonardi. 2018. Efficacy of colostrum replacer versus maternal colostrum on immunological status, health, and growth of preweaned dairy calves. J. Dairy Sci. 101:1344–1354. https://doi.org/10.3168/jds.2017-13032.

McGrath, B. A., P. F. Fox, P. L. H. McSweeney, and A. L. Kelly. 2016. Composition and properties of bovine colostrum: A review. Dairy Sci. Technol. 96:133–158. https://doi.org/10.1007/s13594-015-0258-x.

Meylan, M., D. M. Rings, W. P. Shulaw, J. J. Kowalski, S. Bech-Nielsen, and G. F. Hoffsis. 1996. Survival of Mycobacterium para-

tuberculosis and preservation of immunoglobulin G in bovine colostrum under experimental conditions simulating pasteurization. Am. J. Vet. Res. 57:1580–1585.

Mootse, H., A. Pisponen, S. Pajumägi, A. Polikarpus, V. Tatar, A. Sats, and V. Poikalainen. 2014. Investigation of casein micelle particle size distribution in raw milk of Estonian Holstein dairy cows. Agron. Res. (Tartu) 12:153–158.

Phipps, A. J., D. S. Beggs, A. J. Murray, P. D. Mansell, and M. F. Pyman. 2017. Factors associated with colostrum immunoglobulin G concentration in northern-Victorian dairy cows. Aust. Vet. J. 95:237–243. https://doi.org/10.1111/avj.12601.

Pisponen, A., H. Mootse, V. Poikalainen, T. Kaart, U. Maran, and A. Karus. 2016. Effects of temperature and concentration on particle size in a lactose solution using dynamic light scattering analysis. Int. Dairy J. 61:205–210. https://doi.org/10.1016/j.idairyj.2016.06.006.

Pouliot, Y., and S. F. Gauthier. 2006. Milk growth factors as health products: Some technological aspects. Int. Dairy J. 16:1415–1420. https://doi.org/10.1016/j.idairyj.2006.06.006.

Raimondo, R. F. S., J. S. P. Ferrão, S. I. Miyashiro, P. T. Ferreira, J. P. E. Saut, D. B. Birgel, and E. H. Birgel Junioar. 2019. The dynamics of individual whey protein concentrations in cows' mammary secretions during the colostral and early lactation periods. J. Dairy Res. 86:88–93. https://doi.org/10.1017/S0022029918000808.

Silva-del-Rio, N., D. Rolle, A. García-Muñoz, S. Rodríguez-Jiménez, A. Valldecabres, A. Lago, and P. Pandey. 2017. Colostrum immunoglobulin G concentration of multiparous Jersey cows at first and second milking is associated with parity, colostrum yield, and time of first milking, and can be estimated with Brix refractometry. J. Dairy Sci. 100:5774–5781. https://doi.org/10.3168/jds.2016-12394.

Stott, G. H., D. B. Marx, B. E. Menefee, and G. T. Nightengale. 1979. Colostral immunoglobulin transfer in calves. II. The rate of absorption. J. Dairy Sci. 62:1766–1773. https://doi.org/10.3168/jds.S0022-0302(79)83495-5.

Venkiteshwaran, A., P. Heider, L. Teysseyre, and G. Belfort. 2008. Selective precipitation-assisted recovery of immunoglobulins from bovine serum using controlled-fouling crossflow membrane microfiltration. Biotechnol. Bioeng. 101:957–966. https://doi.org/10.1002/bit.21964.

Zydney, A. L. 2016. Continuous downstream processing for high value biological products: A review. Biotechnol. Bioeng. 113:465–475. https://doi.org/10.1002/bit.25695.

ORCIDS

A. Sats https://orcid.org/0000-0003-0047-2713
T. Kaart https://orcid.org/0000-0002-8936-768X
H. Andreson https://orcid.org/0000-0001-8683-8792
I. Jõudu https://orcid.org/0000-0003-2189-7884